

# Dynamical effects of the long bar in the Milky Way

Esko Gardner<sup>1</sup>, Kimmo A. Innanen<sup>2</sup> and Chris Flynn<sup>1</sup>

<sup>1</sup>Tuorla Observatory, Department of Physics and Astronomy, University of Turku  
Väisäläntie 20, FI-21500 Piikkiö, Finland  
e-mail: esgard@utu.fi

<sup>2</sup>Dept. of Physics and Astronomy  
York University, Toronto, Canada

## Abstract.

We examine the dynamical effects on disk stars of a “long bar” in the Milky Way by inserting a triaxial rotating bar into an axisymmetric disk+bulge+dark halo potential and integrating 3-D orbits of  $10^4$  tracer stars over a period of 2 Gyr. The long bar has been detected via “clump giants” in the IR by López-Corredoira et al. (2007), and is estimated to have semi-major axes of  $(3.9 \times 0.6 \times 0.1)$  kpc and a mass of  $6 \times 10^9 M_\odot$ . We find such a structure has a slight impact on the inner disk-system, moving tracers near to the bar into the bar-region, as well as into the bulge. These effects are under continuing study.

**Keywords.** Galaxy: kinematics and dynamics, Galaxy: center, Galaxy: disk

---

## 1. Introduction

Our initial interest was to study a barred galaxy potential, and especially the resonance effects which might lead to vertical ejection into the halo of globular clusters formed in the disk as suggested by Innanen (2007). We took a triaxial ellipsoid, a Ferrers’ potential, to model the bar (see Pfenninger (1984) for a similar application of the potential as a bar). We decided to look at the effects of the “long bar” described by López-Corredoira et al. (2007), taking their parameters directly, and applying it to our system. The dynamical effects of the bar are quite interesting, and it should be possible to constrain the bar parameters with analysis of these effects.

We also present a brief discussion on the scale-length of the Galactic disk, and a revised version of the Flynn et al. (1996) Galactic disk model with a shorter scale-length of 3 kpc rather than 4.4 kpc, to be more consistent with recent observations.

## 2. Scale-length of the Milky Way disk

Our motivation in constructing a disk model with a revised disc scale-length stems from recent infrared observations, which show a considerably shorter scale-length for the Galactic disk than optical observations. The disk scale-length ( $h_R$ ) adopted in Flynn et al. (1996) was 4.4 kpc, based on the kinematic determination (using velocity dispersions of old disk red giants) by Lewis & Freeman (1989), who obtained a scale-length of  $h_R = 4.4 \pm 0.3$  kpc. It has been long known that the scale-length measured in the infrared is considerably shorter than in the optical, Pioneer 10 data giving  $h_R = 5.5 \pm 1.0$  kpc already in the 1980s (van der Kruit (1986)). More recently near-IR data in J and K with DENIS give  $h_R = 2.3 \pm 0.1$  kpc and 2MASS of K giants gives  $h_R = 3.34 \pm 0.1$  kpc (López-Corredoira et al. (2002), Ruphy et al. (1996), Ojha (2001)). These latter surveys

probe the scale-length of emitted light, mainly by giant stars, rather than probing directly the scale-length of the mass, which is what we are actually interested for modeling the disk’s potential. M dwarfs do trace the mass directly: star-counts with HST in the 1990s of disk M dwarfs indicate a disk scale-length of  $3.0 \pm 0.4$  kpc (Gould et al. (1997)). On the other hand, local kinematics of disk stars, which should also be mostly sensitive to the mass rather than the light distribution, give a range of possible scale-lengths 1.7–2.9 kpc (Bienayme & Sechaud (1997)). Very recently, F to K type dwarfs, for which distances and metallicities have been determined in the huge numbers in 6500 square degrees of sky and probing to distances of up to 20 kpc above and below the disk near the Sun using SDSS data, give a scale-length of  $2.6 \pm 0.5$  kpc (Jurić et al. (2008)).

### 3. The disk model

The Flynn et al. (1996) model of the Galactic disk has a  $h_R = 4.4$  kpc, and is built from three superimposed Miyamoto-Nagai potentials (with different linear scales) to obtain the exponentially falling density profile. In light of recent observations, we would like a shorter disk scale-length, and modified the Flynn et al. (1996) model to a disk with  $h_R = 3.0$  kpc. The local volume density local surface density of the disk are as in the 1996 model (i.e.  $\rho_0 \approx 0.1 M_\odot/\text{pc}^3$  and  $\Sigma_\odot \approx 50 M_\odot/\text{pc}^2$ ), and are consistent with local measurements (Holmberg & Flynn (2000)). We adopt a solar Galactocentric distance of  $R_\odot = 8$  kpc. Figure 1 shows the surface density profile of the disk model, with the dashed line indicating a scale-length of 3 kpc. This is a good fit over a wide range of Galactocentric radii (2 to 15 kpc). Note that the disk truncates strongly at approximately 18 kpc.

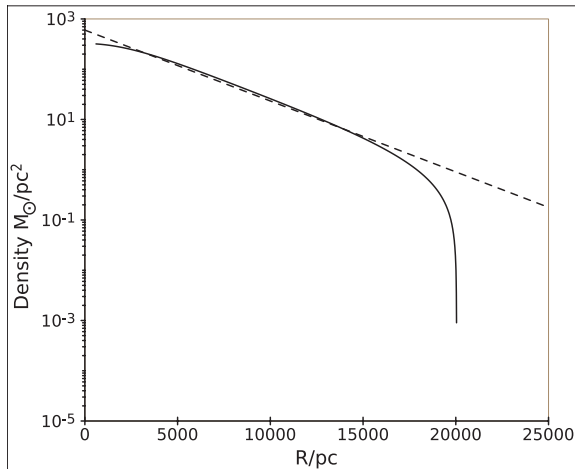


**Figure 1.** The surface density of the disk component as a function of Galactocentric radius. The dashed line corresponds to an exponential density falloff, 3 kpc, which is a good fit to the model over a wide range of radii. Note that the density truncates strongly at 18 kpc.

### 4. Inserting the long bar

We insert a triaxial bar potential into the central regions of the model. We chose a uniform density Ferrers’ potential (see eg. Chandrasekhar (1969), or Binney & Termaine). The linear semi-major axes (3.9:0.6:0.1 kpc), and mass ( $6 \times 10^9 M_\odot$ ) were chosen from

López-Corredoira et al. (2007), who used “red clump” stars detected in a 10 degree wide region observed in the near IR along the Galactic plane. Note that the long bar is very thin vertically, a property which leads to some interesting effects on orbits of disk stars which come near it. The bar is set to rotate around the  $z$ -axis with with a pattern speed of 50 km/s/kpc, giving it a speed of 200 km/s at its tip. This is the speed suggested by OLR (Dehnen (2000)), although we have tried a range of pattern speeds from 0 to 75 km/s/kpc, without substantially altering the conclusions of the paper. The initial phase angle of the bar is as observed by López-Corredoira et al. (2007), i.e. 43 degrees. An important point to note is that we aim to investigate the effects of the “long bar”, rather than the smaller “COBE bar” (Bissantz & Gerhard (2002)), which has dimensions (3.5:1.4:1) kpc, and a position angle of 22 degrees is rather dissimilar to the long bar.

## 5. Disk simulation

We set up an exponential distribution of tracer stars with the same scale-length as the disk. We chose  $U, V$ , and  $W$  velocities from a normal distribution with a standard deviation of 10 km/s around the local standard of rest (i.e. the circular velocity) in the total potential, so that the stars are very nearly on exact circular orbits. Thus the disk is initially inherently cold, and aids in following the secular development of the long bar’s kinematic effects. We integrated the orbits of  $10^4$  objects in steps of  $10^4$  years, with a total time of 2 Gyr, in both the barred and unbarred systems, using the long bar with the parameters advocated by López-Corredoira et al. (2007). We also examined the effects of a thicker, less dense long bar, with an axial ratio of (3.9:2:1) kpc.

## 6. Results and discussion

We present here a preliminary look at the results. In Figures 2, and 3, we show the final distribution of the objects, after 2 Gyr of orbital integrations, for the cases of “no bar”, a long bar of high density ( $6 M_{\odot}/pc^3$ ) and a long bar with a much lower density ( $0.2 M_{\odot}/pc^3$ ). The initial (orange), and final radial distributions of the objects are shown in Figure 2. The vertical distribution is shown in Figure 3. In both, the “no bar” case (cyan), shows little secular evolution, indicating that the disk has been set up in a stable manner. In the denser long bar (magenta), the bar is injecting the inner regions with disk stars from approximately 1 kpc beyond the tip of the bar. Within the bar region, significant modification of the distribution profile takes place, as one would expect. This is seen as a knee in the distribution profile at  $\log R = 3.0 - 3.6$ . The less dense, thick bar (blue), has much smaller effects, with a small knee forming around 1 kpc, which coincides with the spherical area inside the bar.

The bars have almost no effect on the  $z$ -distribution of the disk, there is a slight shift towards higher values in the thin case (magenta), these are mostly tracers that orbitally evolve towards the center of the system, ie. into the bulge. There is no significant ejection to large heights above the disk.

Acknowledgements: We thank Martin López-Corredoira for his useful comments on the manuscript. EG acknowledges the financial support of the Finnish Cultural Foundation, and the Finnish Graduate School in Astronomy and Space Physics. CF and KI are very grateful to the Academy of Finland for financial support.

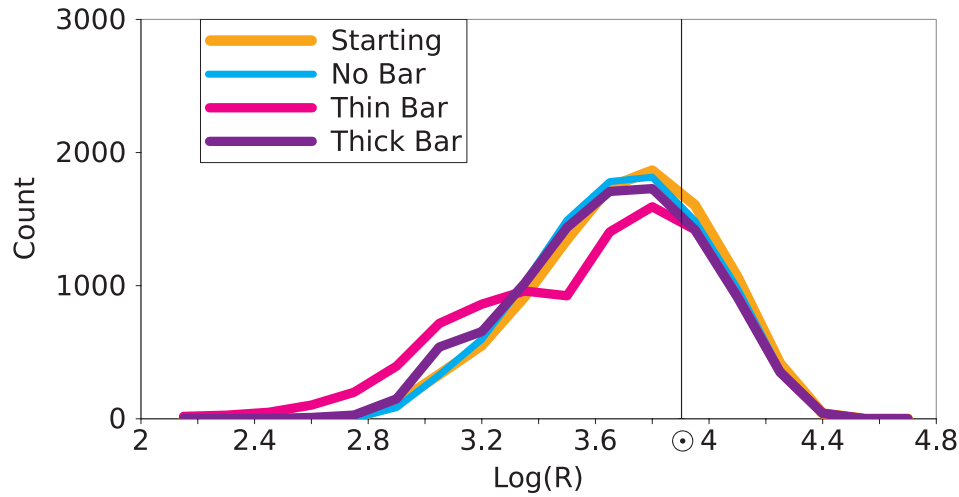


**Figure 2.** Histograms of Galactocentric radii of the tracer stars, for the initial distribution (orange), and after all three simulations have run (2 Gyr). The vertical line marks the position of the Sun at 8 kpc from the Galactic center. The “no bar” case (cyan) shows no secular evolution, indicating the initial setup in the disk is stable. Cases with the bar turned on show some secular evolution. Analysis shows that the long thin bar (magenta) has slight dynamical effects on disk stars which pass near it, injecting the inner disk, and bulge, with stars that have orbits near the tip of the bar. The thicker bar exhibits a feature around 1 kpc.

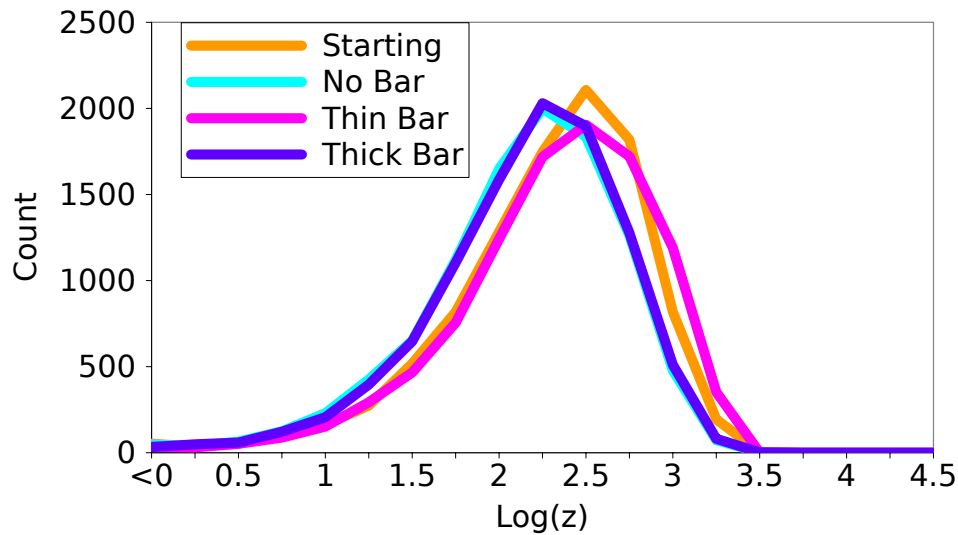


**Figure 3.** Histograms of the vertical height of the tracer stars, initially, and at the end of 2 Gyrs integration, for the “no bar” case (cyan), the long bar and the thicker long bar cases (magenta, blue). No secular evolution is seen in the distributions with the bar, although there is a slight trend to higher  $z$ -values in the thin bar case.

## References

- Bienayme, O. & Sechaud, N. 1997, *A&A*, 323, 781  
 Binney, J. & Tremaine, S. 2008, *Galactic Dynamics 2 ed.*, Princeton University Press  
 Bissantz, N. & Gerhard, O. 2002, *MNRAS*, 330, 591  
 Chandrasekhar, S. 1969, *Ellipsoidal Figures of Equilibrium*, Yale University Press  
 Dehnen, W. 2000, *AJ*, 119, 800

- Flynn, C., Sommer-Larsen, J., & Christensen, P.R. 1996, *MNRAS*, 281, 1027
- Gould, A., Bachall, J. N. & Flynn, C. 1997, *ApJ*, 482, 913
- Holmberg, J. and Flynn, C. 2000, *MNRAS*, 313, 209
- Innanen, K. A. 2007, *CeMDA*, 99, 161
- Jurić, M., Ivezić, Ž., Brooks, A., Lupton, R. H., Schlegel, D., Finkbeiner, D., Padmanabhan, N., Bond, N., Sesar, B., Rockosi, C. M. and Knapp, G. R., Gunn, J. E., Sumi, T., Schneider, D. P. and Barentine, J. C., Brewington, H. J., Brinkmann, J., Fukugita, M., Harvanek, M., Kleinman, S. J., Krzesinski, J., Long, D., Neilsen, Jr., E. H., Nitta, A., Snedden, S. A. & York, D. G. 2008, *ApJ*, 673, 864
- van der Kruit, P. C. 1986, *A&A*, 157, 230
- Lewis, J. R. & Freeman, K. C. 1989, *AJ*, 97, 139
- López-Corredoira, M., Cabrera-Lavers, A., Garzón, F. & Hammersley, P. L. 2002 *A&A*, 394, 883
- López-Corredoira, M., Cabrera-Lavers, A., Mahoney, T. J., Hammersley, P. L., Garzón, F. & González-Fernández, C. 2007, *AJ*, 133, 154
- Ojha, D. K. 2001, *MNRAS*, 322, 426
- Pfenniger, D. 1984, *A&A*, 134, 373
- Ruphy, S., Robin, A. C., Epchtein, N., Copet, E., Bertin, E., Fouque, P. & Guglielmo, F. 1996, *A&A*, 313, 21
- Walterbos, R. A. M. & Kennicutt, Jr., R. C. 1988, *A&A*, 198, 61